Instruments and Experimental Techniques, Vol. 45, No. 2, 2002, pp. 183–193. Translated from Pribory i Tekhnika Eksperimenta, No. 2, 2002, pp. 42–53.

APPLICATION OF COMPUTERS IN EXPERIMENTS

A Technique for Testing the Si Tracker Modules for the D0 Collider Experiment (FNAL) and Comparative Analysis of the Test Results

P. F. Ermolov, E. G. Zverev, D. E. Karmanov, A. K. Leflat, M. M. Merkin, and E. K. Shabalina

Skobel'tsyn Institute of Nuclear Physics, Moscow State University, Vorob'evy gory, Moscow, 119899 Russia

Received June 8, 2001; in final form, August 31, 2001

Abstract—The Skobel'tsyn Institute of Nuclear Physics (SINP) of Moscow State University participates in the development of a silicon tracker for the D0 experiment (FNAL, USA). The SINP specialists were engaged in assembling and testing of the end-disc detectors for the tracker. A technique for testing the disc modules is described, and the test results are presented. They are compared to the disc-detector parameters and measured before the assembling. This comparison can be used to create test procedures and the detector-selection criteria in the development of large-sized tracking systems on the basis of single-sided microstrip detectors.

1. DESIGN FEATURES OF THE END DISCS OF THE SILICON TRACKER FOR THE D0 EXPERIMENT

The Si microstrip tracker [1] for the D0 experiment (FNAL, USA) consists of three main parts (see Fig. 1 in [2]): a central barrel, internal discs, and end discs [3]. All tracker components have a modular structure: the modules of the internal and end discs are shaped as a wedge, and the modules of the central barrel are rectangular. A module contains one Si detector or more and flexible printed-circuit boards with unpackaged chips of the readout electronics.

Each of the four end discs incorporates 24 two-layer wedges; each wedge is composed of two single-sided half-wedges glued together back-to-back. A simplified configuration of the half-wedge is shown in Fig. 1. The silicon detectors for the end discs are single-sided microstrip detectors with p^+-strips in the n-type material with a capacitive readout [3]. Both the inner and outer Si detectors are glued to a Be substrate so that the strips of one detector extend the strips of the other. Another Be plate is glued to the outer-detector face, and a flexible printed-circuit board (FPCB) with six SVX2E chips is glued in turn to this Be plate [4]. The external ends of the inner-detector strips are connected by microbonding to the internal ends of the outer-detector strips, and the external ends of the outer detector are bonded to the appropriate inputs of the SVX2E chips.

In the main, the modules of the D0 silicon tracker were assembled in FNAL with the use of special equipment [5]. With some simplifications, the assembling process for the end-disc wedge consists of (1) gluing the bark side of the outer detector on the Be substrate, (2) gluing the FPCB with the readout chips on the face of the outer detector, (3) connecting the outer-detector strips to the chip inputs by microbonding, (4) precision mounting and gluing of the inner detector, (5) connecting the inner- and outer-detector strips with microbonding, (6) encapsulating the connective wires of the half-wedge with a protective compound, and (7) back-to-back gluing of two half-wedges together.

Most of these operations have no analogs among standard microelectronics processes, because wiring is carried out for unpackaged devices of about 40-cm^2 area, stacked up in several layers; in addition, the number of microbonding connections in one assembly reaches 5000. All these operations call for careful testing of the modules thus produced. While testing, we determine (1) the serviceability of the assembled module, (2) the reliability of its operation, and (3) the number of inoperative channels in the module.

For these problems to be solved, all assembled modules of the D0 tracker were tested. We describe in detail the equipment and the procedure of these tests, and the results obtained for the end-disc modules. Note that the test results of the assembled modules also help optimize the technique for testing the original Si detectors [2, 6]. Moreover, comparing the measured detector data with the test results of finished modules, one can reveal the most hazardous technological operations in the disc assembling.

2. TEST PROCEDURE FOR THE D0-TRACKER COMPONENTS

The test procedure for the tracker modules incorporates three main components [7]: a performance test (so-called functional test), a reliability test (so-called burn-in test), and a laser test.

The serviceability of the boards with readout integrated circuits (FPCB) is tested before their mounting on the detector; hence, these tests are considered to

0020-4412/02/4502-0183$27.00 © 2002 MAIK "Nauka/Interperiodica"

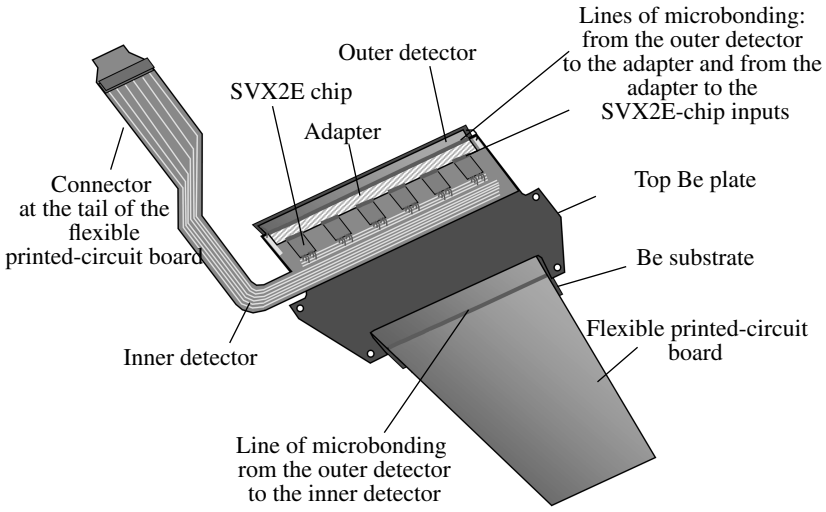

Fig. 1. Simplified configuration of the single-sided half-wedge.

check the normal operation of the detectors and the module after the assembling.

All the tests use the same electronic units; they basically differ in the test duration, the number of devices being simultaneously checked, the testing signal, and the form of data representation.

Figure 2 shows a block diagram of the system, which is common for all test benches for recording the parameters and reading the data out of one tested module. The 128-channel SVX2E chip reads the signals out of the Si-detector strips, amplifies, multiplexes, and digitizes them in a 8-bit analog-to-digital converter (ADC). The result is outputted to the 8-bit parallel data bus in the form of a dependence between the channel number and the pulse height in the channel. The timing system for the data output allows the connection of a few chips to the same data bus.

The SVX2E chip allows to simultaneously change in all channels the gain, the integration time of the output signal, the calibration-signal amplitude, the output for a zero input signal (pedestal), etc. It is necessary to set the chips in the working state before the start-up by loading the appropriate parameters into them. The SASeq unit is used to load the operating parameters and read out the data [8]. One SASeq unit can serve two data buses.

Apart from the data reading and recording, the SASeq offers some services of a control system. It measures the current consumed by the chips and the temperature of the tested module and, through a special interface board (JB), controls the connection of the supply voltages to the module. The JB comprises a few relays, connecting the supply voltages and fuses for each feeder. The SASeq and JB units are made to the VME standard. The SASeq unit is computer-controlled through a standard Bit-3 VME controller [9].

The testing equipment demands three power sources (according to the number of supply voltages for the SVX2E chips) and a bias-voltage source for the detector. Controlled VME4877PS multichannel voltage sources with an internal current meter supply the majority of test benches with the bias voltage. The voltage sources are serviced with a special program independent of the test programs.

2.1. Performance Test

The performance test is used to rapidly check the normal operation of one module during its assembling or repairing. The block diagram of the performance test is similar to the diagram of the testing electronics in Fig. 2. The test checks (1) the total current of the detectors in the module at an operating voltage and (2) the total consumption currents of the SVX2E chips for each of the three voltage supplies. When started, the test loads the operating parameters and, then, reads out the data in a few cycles. The readout cycles can be implemented by applying a calibration pulse of a given amplitude to the input of any channel. The data acquired in the readout cycles are averaged over the number of cycles and tabulated. The table contains the channel number and the average pulse height in the channel and is used to construct a plot. The test results are not saved as a file.

The performance test checks the normal operation of the readout chips and can reveal detector damage if it is associated with the leakage current (the detector cleavage, a deep scratch, or an open-circuit in the high-voltage line or detector ground). Some problems with the individual channels of the detector and electronics can also be detected; however, the reliability of these results is low, because the number of readout cycles is conventionally 100 or less, and only the channels not

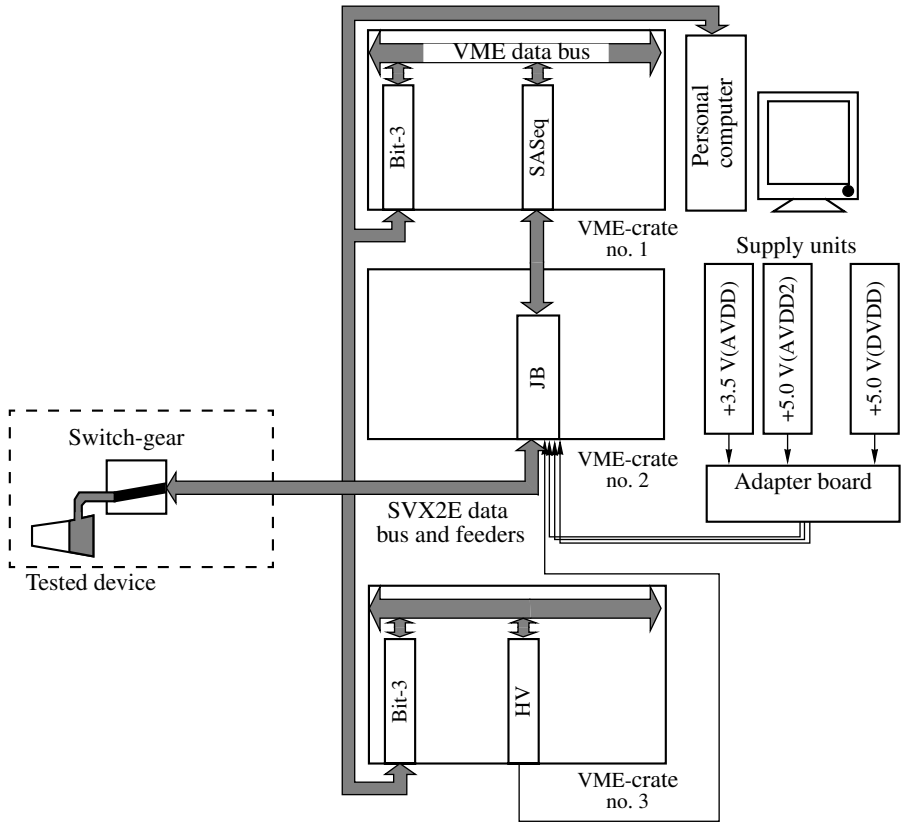

Fig. 2. Block diagram, common for all test benches, of the system for recording the parameters and reading data out of one module.

responding to the calibration signal are reliably detected.

The performance test is carried out without cooling, which limits its duration. The power dissipated by the six SVX2E chips is ~5 W, and, without the use of a special heat sink, the device under test is heated to 50°C within ~10 min, which sharply increases the leakage currents in the detectors and the noise in the readout electronics.

A half-wedge is considered to pass the test if the leakage current of two detectors is other than zero, <20 μA at an operating voltage, and all the chips in the assembly function well.

When checking a double-layer wedge, the performance test is successively carried out with each of its two half-wedges.

2.2. Reliability Test

The reliability test is used to check whether or not the module reliably operates over a few days under near-actual conditions. A block diagram of the reliability test is shown in Fig. 3. Apart from the standard units (Fig. 2), the circuit incorporates a liquid cooling system for the tested devices. This system comprises a cooler; a distributor; and a system of pipes conveying a water-ethylene glycol mixture, cooled to –5°C, to the radiators on which the modules are mounted for testing.

The test bench and software allow for the simultaneous check of up to 16 devices for a few days. The test conventionally lasts 72 h. If defects appear in the tested device in the first run, the device is repaired and put to the second test for 24 h more.

The following characteristics of each module are measured in the routine test every hour: (1) the total leakage current of the detectors at the operating voltage; (2) the total consumption currents of SVX2E chips for each of the three supply voltages; and (3) the device temperature.

A special test that consists of 1000 cycles of module-data readout is done every hour. Some of these cycles are performed without applying the calibration signal, and these data are used to determine the noise level in each channel. In the other cycles, the calibration signals with amplitudes A, $2A$, and $3A$ are sequentially fed into each channel. The data obtained are used to determine the gain in each channel.

The results are presented as (1) plots of the measured current and temperature against time, (2) tables and graphs of noises in the channels as functions of the channel number (in each run), and (3) tables and graphs of the channel gains as functions of the channel number

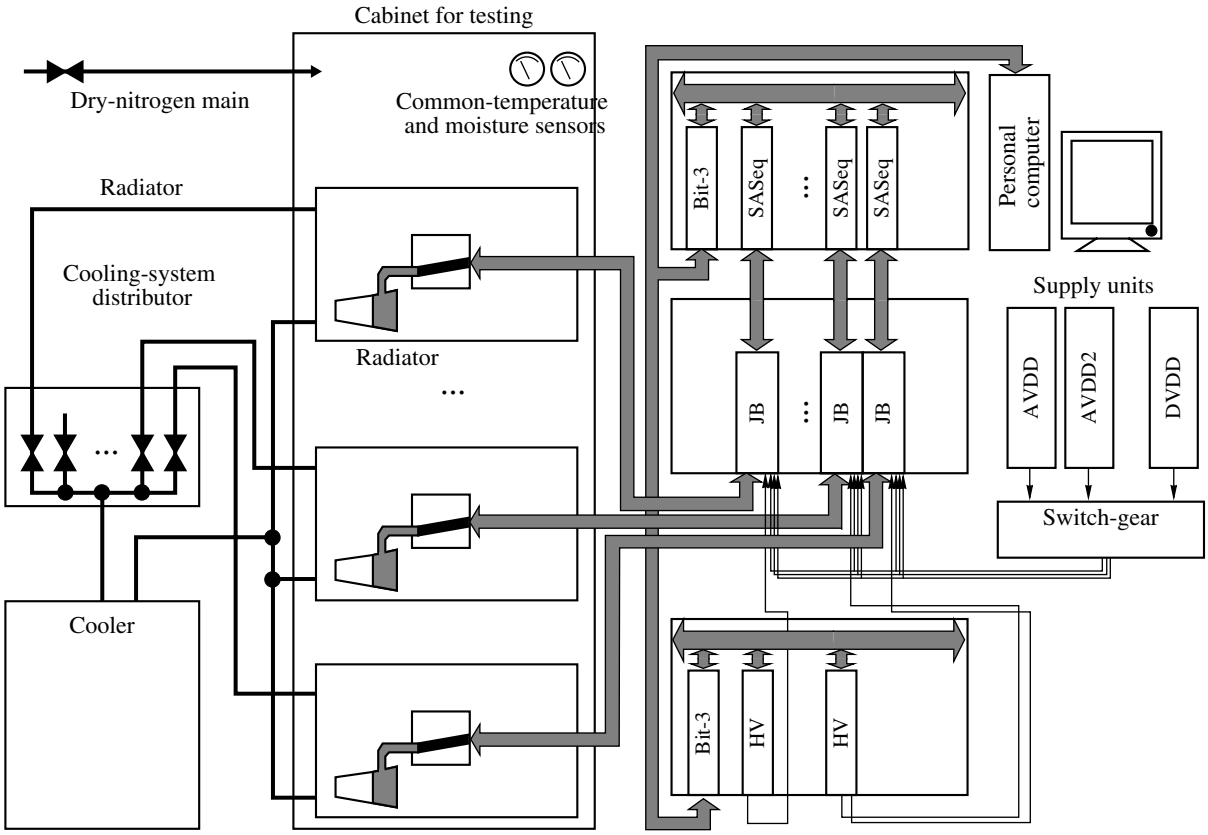

Fig. 3. Block diagram of the reliability test.

(in each run). All the results are stored in data files and are available for subsequent analysis on necessity.

The reliability test provides the knowledge of the reliability of tested devices and helps detect those inoperative. In addition, it permits the determination of the number of problematic channels. Among them are channels with a high noise (>100% above average), channels with a reduced gain (<80% of average), and channels with an increased gain (>30% above average).

The channel noise is defined as a variance of the pedestal amplitude in the channel throughout the data-readout cycles in the given run. In order to eliminate the low-frequency pickup systematically shifting the pedestal in all channels of the module from cycle to cycle, the pedestal values in each readout cycle are normalized by the assembly average before calculating the variance. The normal noise level in the channel is 2–3 ADC counts at the operating temperature.

The reliability test is decisive in determining the amount of noisy channels. The information on the amount and numbers of noisy channels obtained in the reliability tests is definitive for the assembling stage and is entered in the shareable database of the D0 tracker. Typical noise levels in the half-wedge channels are shown in Fig. 4.

As noted, the signal gain in the SVX2E-chip channels is specified while loading the parameters of its operation. However, when a detector is connected to the channel input, the calibration voltage pulse is divided between the strip capacitor and the amplifier input capacitor. As a result, the calibration-pulse height, and, hence, the output-pulse height, significantly decrease. The channel gain calculated in these conditions is also underestimated.

The input amplifier in the SVX2E chip is charge-sensitive; i.e., its input capacitance is theoretically infinite. However, in fact, the gain of the chip with the open feedback circuit is low ($K = 1500$), and the strip capacitance (~20 pF) is comparable with the input channel capacitance. Since the end-disc detectors are shaped as trapezoid and the strips are parallel to its side, the strip lengths and, hence, capacitances differ. In consequence, the measured gain depends on the channel number: channels with larger numbers correspond to shorter strips, and their gains are higher.

These facts make it possible to detect defects in strips and detector bonding. For example, if, for any reason, the amplifier channel is not connected to the detector or the metallization on the detector strip is broken, the input capacitance of the channel amplifier is less and the measured gain in the channel is higher than in the neighbor channels. On the other hand, if two or more strips are short-circuited (on the detector or through the neighbor connections), the input capaci-

tances of amplifiers in the relevant channels are higher and the gain in the channels is lower. A characteristic dependence of the gain, measured in the half-wedge channels, on the channel number is shown in Fig. 5. Channels with a reduced and increased gain are determined with reference to the gain in the neighbor channels.

The half-wedge is considered to pass the reliability test if the consumption of its chips and the detector leakage are stable and lie within the given limits at the operating temperature. In addition, the total number of noisy channels, added to the total number of channels with an increased gain and to the number of channels with a reduced gain, must be under 20 and, after the establishment of the operating temperature, must not increase throughout the test. The operating temperature of a half-wedge is $10 \pm 2°C$; under these conditions, the leakage current of the detectors must be ≤ 5 μA at an operating voltage of 70–90 V.

The half-wedge that has passed the reliability test is not considered to be completely tested; it is subjected to the laser test.

2.3. Laser Test

The laser test is used to detect channels not responding to the signal that is similar to the signal from an ionizing particle. A block diagram of the laser test is shown in Fig. 6. Along with the standard units (Fig. 3), the diagram comprises (1) a semiconductor pulsed laser with a power supply unit, a power system of thermal stabilization, and an optical head for beam focusing; (2) computer-controlled mobile platform to which the tested module is fastened; and (3) synchronization system.

The tested module is fixed on the platform under the optical system to which the laser light is transmitted over the optic fibre. A pulsed laser with a 1064-nm wavelength is used. Radiation with this wavelength penetrates into the silicon through the entire detector thickness [10], generating carries in the silicon, as it is in the passage of an ionizing particle. This signal is collected in a few detector strips and read out by the electronics. The number of activated channels and the signal amplitude in them are governed by the diameter of the focused light spot as well as by the amplitude and duration of the laser pulse.

In the equipment in use, the pulse height at the light-spot maximum exceeds the signal from a minimum-ionizing particle (MIP) about ten times. The laser-pulse duration is 20 ns. The laser spot is about 2 mm in diameter and simultaneously fires about 30 half-wedge channels. A sharper focusing and calibration of the optical system are unjustified, because the same test bench is used for testing modules of different tracker components, located at differing distances from the optical head.

The program controlling the test provides for the initial positioning of the platform with the tested module so that the maximum amount of the laser light is incident on the first strip. In this position, the strip is illuminated 50 times and the signal is read out of the detector after each pulse; then, the platform is displaced by one strip. The cycle is repeated until the last strip is illuminated. The channel number on which the laser-pulse maximum falls at that moment and the signal amplitude in this channel, averaged over 50 pulses, are stored in a file for each platform location. When scanned, the detector is at the operating voltage; the test bench is isolated from the external light sources. A characteristic pattern of the response of the half-wedge channels to the laser pulses is shown in Fig. 7. The test bench and software permit simultaneous testing of one module.

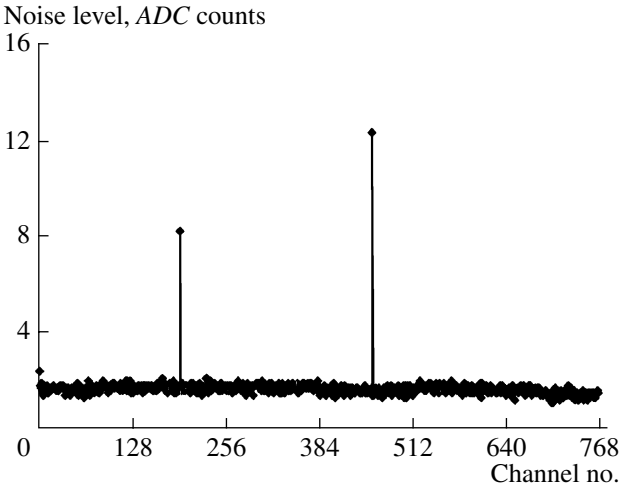

Fig. 4. Amplitude of the noise in the channels of the HCA-133 half-wedge. Increased background in channels 194 and 459.

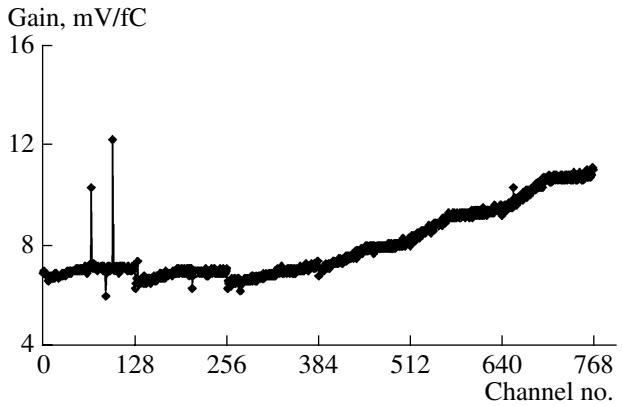

Fig. 5. Amplification in the channels of HCA-133 half-wedge. Increased gain in channels 68 and 98; reduced gain in channel 88.

The detector-channel operation is considered to be normal if the measured signal from the laser-pulse maximum in this channel is 70% of the detector aver-

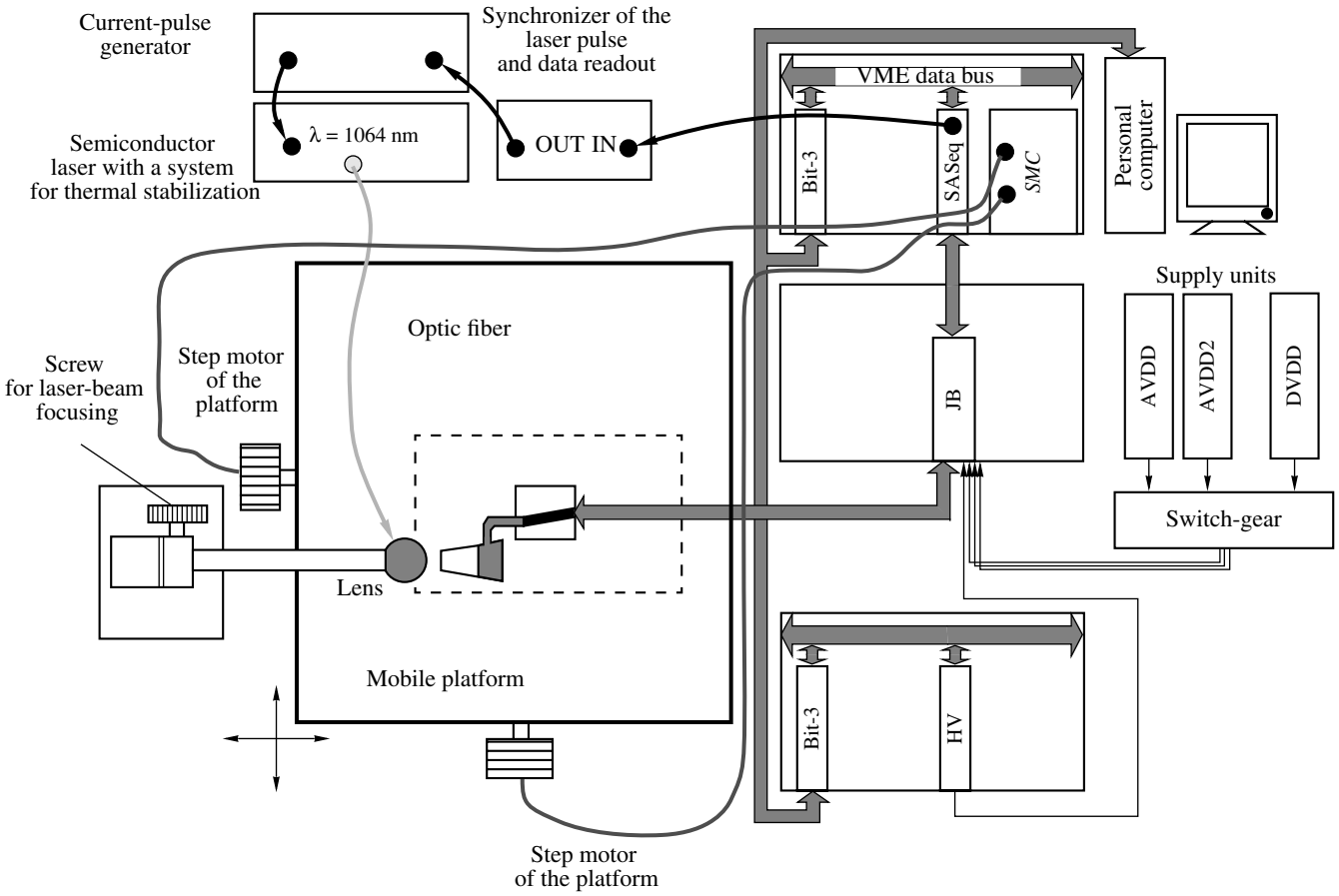

Fig. 6. Block diagram of the laser test: (*SMC*) step-motor controller.

age or more. If the signal is below this value, the channel is considered to be dead. The information on the dead channels found in the laser test is final for the assembling stage and is entered into the Si-tracker database. While testing the half-wedges, the laser scanned the detectors following two paths along the base of the detector trapezoid (Fig. 1). The first path ran along the wider base of the outer detector in the assembly, and the other path ran along the wider base of the inner detector. The dead channels, attributed to the broken strip metallization, and channels with defects of microbonding of the inner detector on the outer one were thus revealed.

Consider in more detail the causes for the dead channel to appear: (1) short-circuits in the bonding, metallization, or implantation of the neighbor strips; (2) breakdown or a significant leakage of the strip's blocking capacitor; (3) improper bonding of the amplifier channel on the strip; (4) improper bonding of the inner-detector strip on the outer one; (5) breaks in the strip metallization; and (6) inoperative amplifier channels.

When a particle is incident on the detector, the charge is predominantly collected into one strip. In this case, a short-circuit of two strips causes the collected charge to halve between the strips and the output signal in the short-circuited strip decreases by ~50% of normal. However, in this case, the laser spot is rather wide and the charges collected from the laser pulse in the neighbor strips are almost equal. As a result, if the neighbor channels are short-circuited, the redistribution of the charge collected in the laser test is minimal, and the decrease in the signal is virtually insignificant.

A breakdown or significant leakage of the strip's blocking capacitor causes the strip-leakage current to run into the amplifier channel. If the leakage current is sufficiently high, the amplifier channel is overloaded and becomes insensitive to the input signal; the channel is dead.

Apart from detecting the dead channels, the laser test makes it possible to measure the voltage dependence of the leakage current and the full-depletion voltage of the detectors in the tested module. The leakage currents are measured at room temperature (about 20°C) without cooling the device under investigation. Therefore, these currents should be higher than those measured in the reliability test and approximately equal to the currents measured in the detectors before mounting [6] and in the performance test. The leakage current

is taken to be normal if it is under 20 μA and above 100 nA; the latter ensures that there is no break in the bias voltage circuit.

Consider in more detail the technique used in the laser test for determining the full-depletion voltage. For the full-depletion voltage U_{fd} to be measured, the platform with the module under testing is placed so that the laser pulse is incident onto the detector center, if possible, in the region without dead channels. The size of the cluster of strips fired by the laser in the given position is determined at an operating voltage of 70 V. The strip is considered to be fired if its response to the laser pulse exceeds 10% of the maximum amplitude in the cluster. The detector-bias voltage is then reset to 0 V.

After a certain delay (as a rule, 1 s), the voltage starts increasing; a voltage range of 5–120 V with a 5-V step is conventionally used. For each voltage value, 100 laser pulses illuminate the detector, and its response is read out 100 times. The average outputs of the strips included in the cluster are added together and saved in a file. A characteristic voltage dependence of the total amplitude over the cluster is given in Fig. 8b. The detector is considered to be fully depleted when the total amplitude over the cluster levels out. The operating voltage is defined as the full-depletion voltage U_{fd} plus 15 V. The operating voltage thus obtained is entered into the Si-tracker database and has to be used while the device is in service.

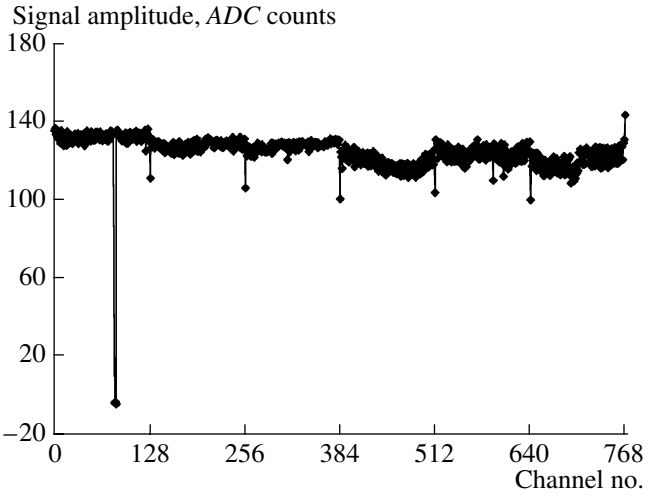

Fig. 7. Amplitudes of signals from the outer detector of the HEA-128 half-wedge in response to laser pulses. Channels 79, 80, and 81 are dead. Channels whose signal amplitude is decreased and numbers are multiples of 128 are the normal detector channels connected to the outer channels of readout integrated circuits.

3. TEST RESULTS FOR THE ASSEMBLED SINGLE-LAYER HALF-WEDGES. COMPARISON WITH THE PARAMETERS OF END-DISC DETECTORS BEFORE THE ASSEMBLING

3.1. Measured Parameters of End-Disc Detectors Before the Assembling

Details of the detector-testing procedure are described in [6]. We consider the experimental results for the detector parameters that either were subsequently measured with the assembled modules or governed the disc parameters measured in the tests from Sections 2.2 and 2.3.

The average leakage current of good end-disc detectors after the assembling was 1.1 μA or 30 nA/cm^2 at an operating voltage. The operating voltage of each detector was defined as the full-depletion voltage for this detector plus 15 V. A characteristic voltage dependence of the current is shown in Fig. 9. The majority of detectors exhibited an increase in the current at voltages above the depletion voltage, which may be attributed to the defects at the rear side of the wafer.

The average full-depletion voltage, measured after fabricating the detectors, was 39.5 V (Fig. 10). The measurements were carried out by the $1/C^2$ technique with the test structures located at the edges of the wafers on which the detectors were produced [6]. This value corresponded to the resistivity range of the silicon in use. The certified resistivity value of the silicon by Wacker Siltronix was 6 ± 2 kΩ cm. A tail in the distribution at higher depletion voltages was due to the fact that, probably, the silicon batch included a few wafers with a reduced resistivity (about 15 per 1500 wafers).

The average number of capacitors with a leakage >10 nA at 60 V in the good detectors was 1.7 capacitor per detector.

3.2. Comparing the Total Leakage Currents of Detectors

Since the total currents of the detectors after their production are measured at a temperature of 22 ± 2°C, these results should be compared to the values obtained in the laser test that is conducted at the same temperatures. According to the values of total leakage current measured in the laser test, the currents of the detectors mounted on the half-wedges are 3.1 μA per detector, being three times as high as the leakage before the wiring. Analyzing the graph of the current versus voltage (Fig. 9), specifically, an abrupt increase in the current at voltages above the depletion voltages, it is possible to assume that this increase is due to the carrier generation by the rear side of the module detectors. This effect is also observed before the mounting but it is less pronounced. After the mounting, in particular, after cementing the detectors on a rigid Be substrate, the current generation is enhanced through the bending of the detectors by the substrate, because both the detectors and substrates are conventionally not flat, but convex or concave within the limits of 50 μm.

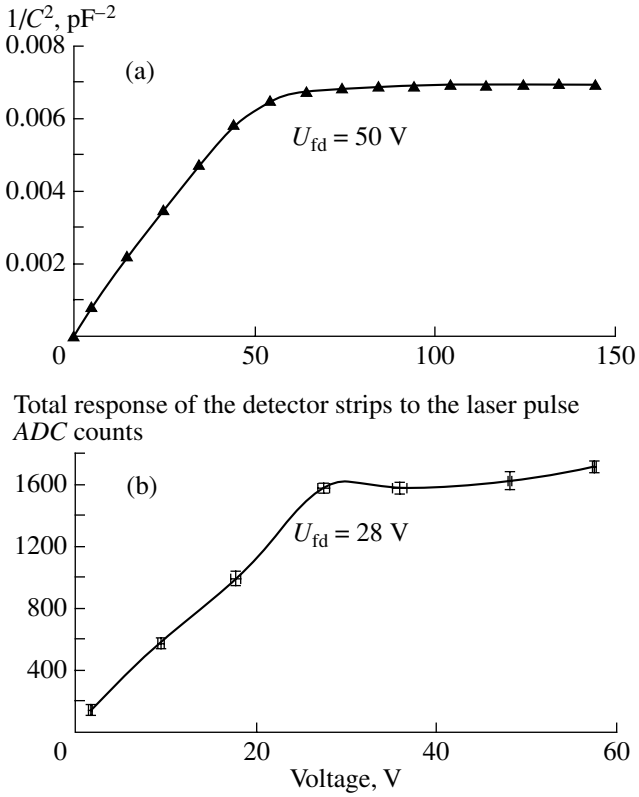

Fig. 8. Characteristic voltage dependence of (a) $1/C^2$ parameter for the test structure of detector 1324 and (b) responses of the outer-detector strips to the laser pulse for the HEA-128 half-wedge.

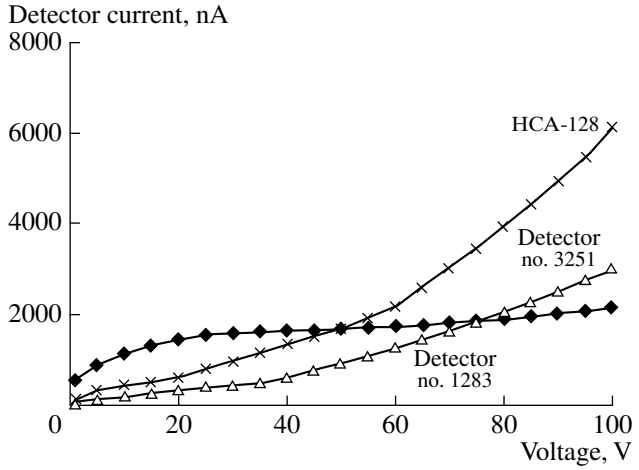

Fig. 9. Characteristic voltage dependences of the line current of detectors 1283 and 3251 (before mounting them in the HCA-128 half-wedge) and the HCA-128 half-wedge after its assembling.

3.3. Comparison of the Depletion Voltages Measured with the Test Structures and Laser Setup

The full-depletion voltage, measured with the laser setup, correlates with the depletion voltages determined with the test structures of detectors by the $1/C^2$ technique (Fig. 11). However, the difference between the depletion voltages obtained in two ways is 10 V on the average and can reach 35 V. Analyzing the distribution of the difference between the depletion voltages measured by the two methods (Fig. 12), we see that we have to use a random deviation instead of a systematic shift of the results obtained using the same method with respect to those obtained in the other way.

In this case, the significant difference in the results may be caused by the nonuniformity of the Si resistivity over the wafer diameter for a large portion of wafers from the lot. The depletion voltage is measured in the test structures located at the periphery of the Si wafer about 1.5 cm from the edge; hence, it may differ widely from the depletion voltage values obtained with the laser setup, since they are measured at the center of the detector, i.e., at the center of the wafer.

According to the Wacker Siltronix specifications, the resistivity deviation over the wafer diameter was within 1.5 kΩ cm with an average resistance of 6 ± 2 kΩ cm in the entire lot. In this case, the difference in the depletion voltages over the wafer diameter reaches ±6, ±15, and ±25 V for wafers with the depletion voltages at the center of 30, 50, and 70 V, respectively. These data are inadequate for the observed spread in the values to be explained, especially for a depletion-voltage range of 30–35 V. However, we cannot exclude the fact that a portion of Si wafers exhibited a nonuniformity in the resistivity of >1.5 kΩ cm. In addition, the accuracy in determining the depletion voltage by the $1/C^2$ and laser-test techniques is within ±5 V (Fig. 8).

If the difference between the results of these two methods is basically attributed to the Si inhomogeneity, the accuracy in determining the depletion voltage by the $1/C^2$ technique can be improved. With this aim in view, we should measure the capacitance of the detector itself instead of the test-structure capacitance; then, the effect of the Si-edge inhomogeneity is less pronounced. This technique for measuring the detector-depletion voltage, perhaps, will be used for the ATLAS detectors.

3.4. Correlation of the Noisy Channels Detected in the Reliability Test with the Measured Leakage Currents

The measured leaks of strip *p–n* junctions show that some strips with a leak coincide with the noisy channels detected in the reliability test. However, the percentage of these coincidences is extremely low: <0.5% of all strips with a leak above 50 nA are more noisy than the normal channels. In the cases where the strip with a high *p–n*-junction leakage produces much noise, the noise profile in the module channels obtained in the reliability test has a characteristic shape (Fig. 13). In Fig. 13, channel 353 with the highest noise corresponds

to the strip with a 350-nA leakage and the neighbor strips exhibited normal currents of about 0.5 nA.

We suppose that, at a strip leakage of about 500 nA, the shot noise due to the current through the *p–n* junction of the strip is responsible for the channel noise. The noise level depends on the integration time selected for the input charge in the SVX2E-chip channel [4]. At a 500-nA current, this addition is about 0.2 fC, which corresponds to 5% of the signal due to MIP in a 300-μm-thick detector. As noted, the average noise level for a half-wedge is 2–3 *ADC* counts, which also accounts for ~10% of the signal from MIP [11]. Hence, the noise in the channel with a 500-nA leakage is $\sqrt{0.05^2 + 0.1^2} = 0.11$ MIP; i.e., it exceeds the common noise level only by 10%.

This approach fails to explain neither the abnormally high noise level (about 0.8 MIP signal, Fig. 13) nor the occurrence of a wide noisy cluster instead of one noisy channel. Thus, the mechanism of the occurrence of channels that are leaky and noisy at a time is not clear, because it is impossible to measure the strip currents in the finished half-wedge. In addition, the statistic is very low: 3 coinciding channels of about 300 leaky and 170 noisy channels.

The analysis of the measured strip-capacitor leaks has also revealed a few coincidences of these strips with the noisy channels in the reliability test. These coincidences are associated with the prebreakdown state of the strip capacitor. In this case, the leakage through the capacitor is not stable, which looks like a noise in the channel. However, the duration of the prebreakdown state is short. In the course of the reliability test (72 h), all capacitors with such a noise were broken down. As a result, at the end of the reliability test and during the laser test, these channels seemed to be dead.

3.5. Correlation of the Dead Channels Found in the Laser Test with the Capacitor-Leakage Currents

As the measurements of the strip-capacitor leaks show, a major portion of the leaky capacitors coincides with the dead channels detected in the laser test. The comparison results are presented in the table.

The first result is the fact that only 12–15% of dead channels found after the assembling in the laser test were defective (leaky) in the measurements of the capacitor leaks in the detectors. This implies that the major portion of dead channels (>80%) appeared during the mounting.

The microbonding of the detector strips on the preamplifier was a serious problem of the assemblage. We used ultrasonic bonding with Al wire of 25.4-μm thickness. A portion of capacitors was assumed to be damaged in microbonding and broken down when turned on. Note that it is difficult to select a force with which the machine presses the wire to the bonding area, because, on the one hand, the force should be sufficient

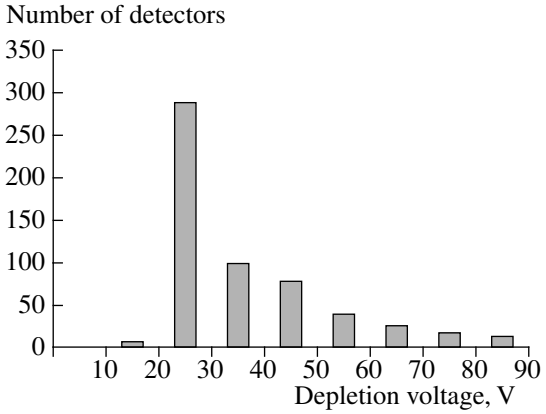

Fig. 10. Distribution of good detectors in the depletion voltage.

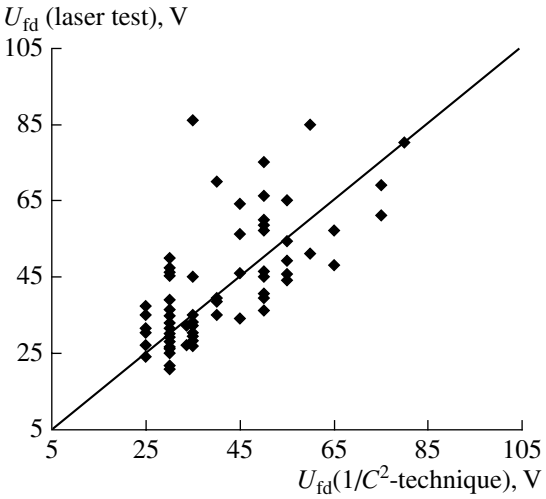

Fig. 11. Correlation between the depletion voltages of the detectors, measured by the $1/C^2$ technique with the test structures, and the depletion voltages measured with the laser setup.

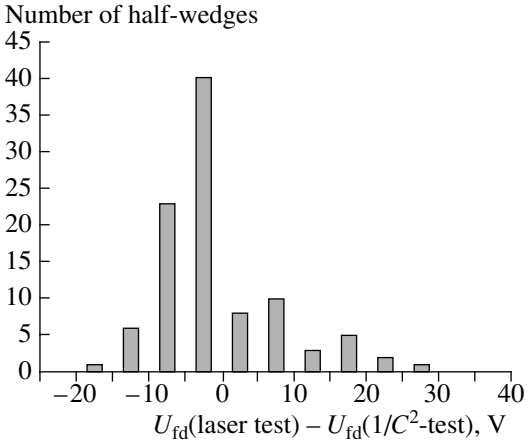

Fig. 12. Frequency distribution of differences between the depletion voltages measured with the laser setup and with the test structures by the $1/C^2$ technique.

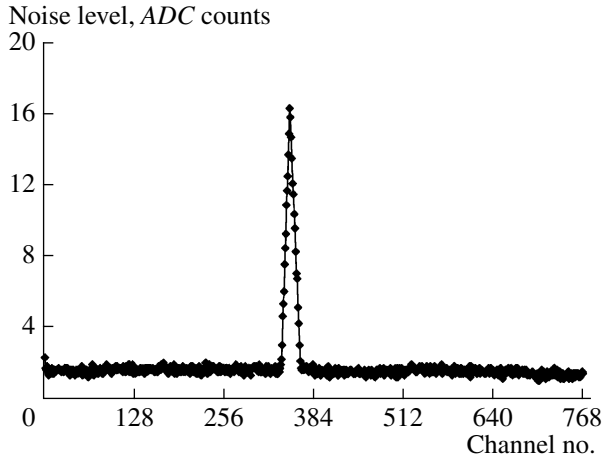

Fig. 13. Cluster of noisy channels of the HCA-052 half-wedge. The cluster has a maximum in the channel 353.

for the bond to be strong; on the other hand, if the force is too strong, the machine crushes the capacitor dielectric. Incidentally, if the detector surface is polluted, the bond strength decreases. In this case, for the appropriate strength to be achieved, the force should be increased, which may cause the dielectric to damage.

The results of this comparison allow us to select the criterion for determining the defect capacitors. We see that the capacitors with a high leakage at low voltages (the first criterion from the table) correspond to the dead channels with a 84% probability. At the same time, the capacitors with a leakage appearing only at a high voltage (the fourth criterion) do not virtually produce dead channels (0.6%). In this case, making the selection criterion more stringent does not virtually lead to a decrease in the number of dead channels in the finished assembly.

We think that this results from the fact that a very low voltage is applied to the blocking capacitors in the end-disc detectors in their operation. Since a capacitor plate is grounded through the polysilicon resistor and the other plate is connected to the amplifier input, the capacitor voltage is equal to the voltage drop across the resistor due to the strip-leakage current. This voltage is $0.5\ \text{nA} \times 1\ \text{M}\Omega = 0.5\ \text{mV}$ on the average for a detector before irradiation. After a two-year operation and receipt of a ~1-Mrad dose, the strip current will increase to 1 μA and the voltage will reach ~0.5 V. With this voltage being so low, dead channels are produced, in the main, by the capacitors having through holes in the double-layer dielectric, which corresponds to the first selection criterion from the table. In addition, some dead channels are produced by capacitors whose dielectric is in the prebreakdown state at 30 V (the second and third criteria), but their contribution is much smaller.

Comparison of the dead channels found in the laser test and the channels with defective blocking capacitors. The total number of tested strips is 142000

Diagnoses and selection criteria		Number of strips with bad capacitors for different selection criteria	Percentage of strips with bad capacitors found to be dead in the laser test of the total number of strips with bad capacitors	Percentage of strips with bad capacitors occurred to be dead in the laser test of the total number of dead strips found in the laser test
No. 1: through holes in both dielectric layers; breakdown from 0 V	At 30 V $I > 100$ nA and at 60 V $I > 100$ nA	129	83.8	13.0
No. 2: holes in one of the dielectric layers (probably, SiO_2); dielectric breakdown at ~60 V and on	At 30 V $I > 10$ nA and at 60 V $I > 100$ nA	33	36.8	–
No. 1 or no. 2	At 60 V $I > 100$ nA	162	73.2	14.7
No. 3: many holes in one of the dielectric layers (probably, Si_3N_4); leakage through the dielectric starts at ~30V, but there is no breakdown up to 60 V	At 30 V $I < 10$ nA and at 60 V 50 nA $< I <$ 100 nA	16	37.5	–
No. 1, or no. 2, or no. 3	At 60 V $I > 50$ nA	183	70.1	15.4
No. 4: holes in one of the dielectric layers (probably, Si_3N_4); the dielectric becomes leaky only at >60 V; no breakdown	At 30 V $I < 10$ nA and at 60 V 10 nA $< I <$ 50 nA	148	0.6	–
No. 1, or no. 2, or no. 3, or no. 4	At 60 V $I > 10$ nA	331	38.7	15.8

CONCLUSION

Comparing the defective channels of assembled modules to the defective strips found on the detectors after their manufacturing helps optimize the process of mass detector testing [5] and develop more rational criteria for estimating the detector quality.

In particular, we suppose that measuring the leakage currents of each strip in each detector is inexpedient, because too small of a portion of leaky strips determined in these measurements actually affects the noise of the assembly.

It is also possible to more precisely formulate the selection criterion for strips with defective capacitors. For single-sided strip detectors whose strips will be grounded, it is necessary to check the capacitor leakage over a 1- to 10-V range. At the same time, testing at a voltage above 50 V provides no additional information on bad channels, but may cause capacitors of normal strips to break down.

ACKNOWLEDGMENTS

The work was supported by the CRDF foundation, grant RE 2-142, 1996–1998.

REFERENCES

1. *D0 Upgrade Collaboration*, *D0 Note no. 2169*, Batavia: FNAL, 1994.
2. Ermolov, P.F., Voronin, A.G., Karmanov, D.E., *et al.*, *Prib. Tekh. Eksp.*, 2002, no. 1.
3. Ermolov, P., Merkin, M., Shabalina, L., *et al.*, *Preprint of Institute of Nuclear Physics, Moscow State Univ.*, Moscow, 1997, no. 97-22/473.
4. Yarema, R., *FERMILAB-TM-1892*, Batavia: FNAL, prepared 1994, revised 1996.
5. Zverev, E.G., Karmanov, D.E., Kubantsev, M.A., *et al.*, *Preprint of Institute of Nuclear Physics, Moscow State Univ.*, Moscow, 2001, no. 2001-28/668.
6. Ermolov, P.F., Voronin, A.G., Karmanov, D.E., *et al.*, *Preprint of Institute of Nuclear Physics, Moscow State Univ.*, Moscow, 2001, no. 2000-15/619.
7. Asman, B., Clark, A., Gerber, C., *et al.*, *D0 Note no. 3841*, Batavia: FNAL, 2001.
8. Gonson, M., Rapidis, P., Yutas, V., *et al.*, *D0 Engineering Note no. 3823.110-EN-504*, Batavia: FNAL, 1999.
9. BIT-3: http://www.sbs.com/pdfs/617ds_cp.pdf.
10. Sze, S.M., *Physics of Semiconductor Devices*, New York: Wiley, 1981, vol. 1. Translated under the title *Fizika poluprovodnikovykh priborov*, Moscow: Mir, 1981, vol. 1.
11. Roco, M., *D0 Note no. 3405*, Batavia: FNAL, 1998.